Framework of the kinetic analysis of O_2-dependent oxidative biocatalysts for reaction intensification

Alvaro Lorente-Arevalo[1], Miguel Ladero[1], Juan M. Bolivar[1]

[1] Chemical and Materials Engineering Department, Faculty of Chemical Sciences, Complutense University of Madrid, Madrid, 28040, Spain

Corresponding author: Juan M. Bolivar (juanmbol@ucm.es)

ABSTRACT

The application of oxygen-dependent enzymes is limited by the low oxygen solubility, a fact that hinders the full operational exploitation of the enzyme activity. This oxygen limitation also creates a difficulty for understanding the intrinsic enzyme kinetics, a critical aspect for the process implementation of oxidative enzymes. Kinetic analysis of O_2-dependent enzymes is a case of ping-pong bi-substrate reaction kinetics but with the added feature of a fixed low concentration of oxygen dissolved in the liquid medium. We propose an analysis framework based on a combination of differential methods (based on initial reaction rates-concentration plots) to analyze the main substrate dependency, while the subsequent integral method (consumption time courses of oxygen dissolved) serves to analyze the oxygen dependency. The methodology is applicable by using the oxygen initially dissolved and only working with liquid suspensions. The analysis was applied to paradigmatic case studies with importance in modern green biooxidations. The modeling framework was validated and applied in scale-up reactions in an instrumented aerated stirred tank reactor.

Table of contents

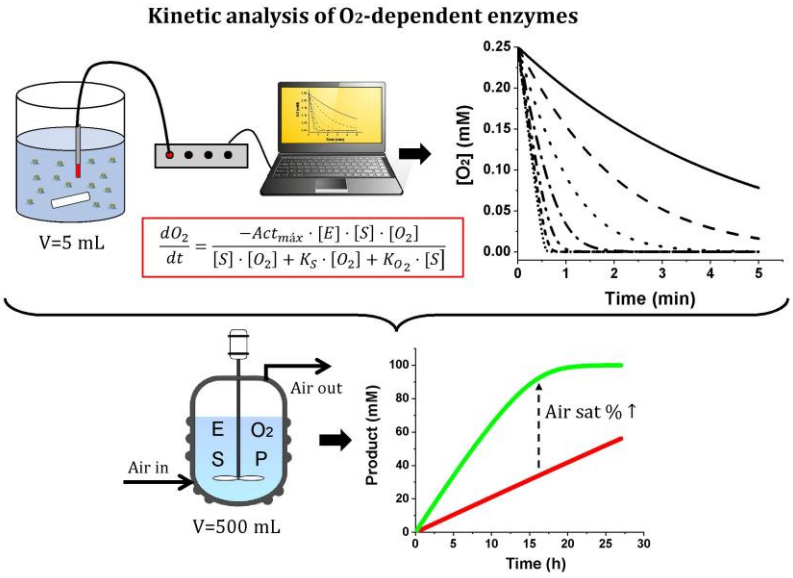

TOC text: Kinetic modelling of O_2-dependent enzyme catalyzed reactions is effectively elucidated from measurements of consumption rates of the initially dissolved O_2 in homogeneous liquid phase. A framework for kinetic analysis and evaluation of the reaction intensification was developed.

Keywords: biooxidations; enzyme activity, applied kinetics, enzyme kinetic; chemical reaction engineering, biooxidation chemistry

INTRODUCTION

Oxidations are one of the most important transformations in the chemical industry. Besides well-established transformations in pharmaceutical and fine chemistry, oxidations are key reactions in the processing, valorization and upgrading of renewable feedstocks in integrated biorefineries [1–4]. Although chemocatalytic methods for performing oxidations are widely used in multiple applications and using raw material from different sources [3–5], oxygen-dependent enzymes [4,6–8] constitute alternative catalysts that can perform biooxidations with exquisite selectivity and under mild conditions compared to chemically catalyzed reactions [2,4,5]. Enzymatic oxidation is particularly attractive because it allows the use of molecular oxygen as the oxidant, under mild conditions, being oxygen the most efficient oxidant agent in terms of atom economy [4].

Oxygen-dependent oxidative enzymes fall under several classes as oxidases, mono- and dioxygenases and, within oxygenation or dehydrogenation mechanistic principles, they catalyze a broad repertoire of interesting reactions as aldehyde formation, hydroxylation, carboxylic acid formation, lactone production… [3–6,8,9]. However, the fascinating promising chemistry also requires careful reaction engineering [10]. Process development for biocatalytic reactions is a complex task that moves from screening of biocatalyst and preliminary characterization to identification of bottlenecks and implementation. In oxygen -dependent enzymes, there is a lack of standardized procedures for guiding development and for identifying the major process limitations in these systems. A useful approach for the study and development of oxidative biocatalytic reactions would be the application of chemical reaction engineering (CRE) principles [11,12]. CRE is interested in elucidating the reaction kinetics based on the determination of the fundamental influencing variables and their effects on the temporal evolution of the composition of a reacting system [11–16]. The understanding of enzyme kinetics is thus used to determine the potential of enzymes to satisfy determined production targets, anticipation of implementation bottlenecks, and for the design of the reactor [16–18]. Moreover, recently, (bio)catalysis is very much in line with a new paradigm in chemical technology: process intensification [19–22]. In this regard, CRE tools applied to the determination of enzyme kinetics are of utmost importance for an optimal exploitation of enzymes via optimization of the biocatalyst and of the operational conditions of such catalysts to enhance process productivity [10,13,15,23].

The development of enzyme-catalyzed oxygen-dependent oxidations encounters traditional and complex challenges due to limitations of activity and stability under operating conditions [10,14,24–26]. Regarding activity, one of the main limitations deals with the need of external oxygen supply, whose transfer rate determines the maximum oxygen concentration achievable into the reactor [13,14,27,28]. Oxygen transfer rate is limited by the solubility of oxygen in aqueous medium and by operational and design aspects of the reactor as mass gas flow and fluid dynamics (e.g. stirring in stirred tank reactors) [13,15,22,29,30]. As a consequence, it is usual that the reaction proceeds with oxygen

concentration below the saturation and the efficiency of use of the enzyme is low [10, 14,16,17,30–32]. These conclusions are clearly important for industrial operation, but they may also have implications for laboratory scale screening of new biocatalysts. The quantification of the enzyme kinetics is implemented by the elucidation and building the kinetic model. For a two-substrate reaction such as an oxidase the reaction rate is best described by the ping-pong bi–bi reaction mechanism [10, 33], Eq 1.

$$R = -\frac{dS}{dt} = -\frac{dO2}{dt} = \frac{Act_{max}\cdot[E]\cdot[S]\cdot[O_2]}{[S]\cdot[O_2]+K_S\cdot[O_2]+K_{O_2}\cdot[S]} \qquad \textbf{Eq 1}$$

Eq 1 gives the reaction rate provided per an enzyme concentration *[E]* for a given set of both substrates. Act_{max} is the maximum specific reaction rate provided by the enzyme at saturating concentrations of both substrates, and it expresses, therefore, the maximum potential of an enzyme to catalyze a reaction with a certain velocity. K_S and K_{O2} are the intrinsic Michaelis constants of each substrate for each enzyme. In applied enzyme kinetics, the enzyme activity is simply a specific reaction rate under defined conditions where the reference is a certain amount of the enzyme. When *[S]* and $[O_2]$ differ from saturating conditions, the specific reaction rate not only differs from the Act_{max} but also from the specific activity under those standard conditions. When the reaction proceeds over time (in a discontinuous stirred tank reactor) or along the reactor (in a continuous flow reactor or the tubular or column type) the velocity decreases, due to consumption of reagents, corresponding to the expression Eq 1. The elucidation of Eq 1 is, therefore, important, not only to achieve full exploitation of *E* but also to predict reactor performance and the needed O_2 external supply rate. *Eq 1* does not include inactivation phenomena. In case that enzyme inactivation takes place, it would also influence the decrease of the reaction rate reaction rate, this would be manifested in a decrease of the population of active enzyme (*[E]*) or time-dependent reduction of the kinetic constant.

Several methodologies have been used to study biooxidation kinetics and to quantify the parameters of *Eq 1*. One common procedure is the measurement of initial reaction rates at different substrate concentrations at fixed initial oxygen concentrations [33]. This analysis can be complemented by varying initial oxygen concentration dissolved in the liquid, but it requires careful control of the oxygen dissolved, which is difficult in conventional spectrophotometer cuvettes or lab vials. Another alternative is based on a semicontinuous stirred tank reactor configuration, whereby initial reaction rates are measured at varying substrate concentrations using a continuous supply of air bubbles, as well as aeration by agitation. Technically, the set-up is closed regarding exchange of substrate, but external supply of air is used. One common complication is the lack of stability of free oxidative enzymes in the presence of gas-liquid interfaces. New methodologies based on advanced reactor engineering have been established by Woodley and coworkers in the last years [13-18,23,28]. One experimental methodology consists in the quantification of oxygen consumed by oxygen mass balance measured by online gas-phase analysis. The method was successfully validated and demonstrated by using two model reactions [10,15,18]. In another set-up the established tube-in-tube reactor technology has been adapted. Here,

the gas phase, at various partial pressures of oxygen, was supplied via an outer tube and allowed to cross a gas-permeable membrane to an inner tube, containing enzyme and substrate solution. The reactor has been developed to operate with ramp kinetics (in the dispersed flow mode) [16].

Another set of methodologies are based on the progress curve analysis. Data points of the reaction progress are obtained to nearly full conversion of substrates, and the set of data concentration-time are analyzed. Reaction progress with numerous data points allows a deeper evaluation of the biocatalyst performance, discrimination of model and identification of stability/inhibition bottlenecks [18]. Deep understanding of kinetics, however, requires enough data points to capture the dependence of one or more substrates [23]. This reduces the number of experiments to be performed because multiple data points can be obtained at once. Progress curve analysis of enzymatic reactions can be performed using either algebraic or dynamic parameter estimation [34]. If the estimation of algebraic parameters is applied, the concentration data must be differentiated to obtain reaction rates [18,23,34]. Acquisition of data points in the time course requires suitable online analytics. Additionally, in oxygen-dependent reactions, full conversion courses of substrates require continuous supply of oxygen, this needed to be achieved avoiding enzyme inactivation and using suitable set-up [29].

In this article, a robust methodology in conventional lab set-up is developed and proposed for estimating the parameters in the biocatalytic reaction kinetic expressions. The methodology determines the parameters in a systematic manner by exploiting the best features of several of the current approaches. The methodological principle is the measurement of the consumption rates of the oxygen initially dissolved in a closed stirred tank reactor (batch configuration) operating in a homogeneous liquid. The analysis is divided in different steps, first we observe maximum initial reaction rates upon main substrate variation. Second, we analyzed the shape of the curve of oxygen consumption courses to predict oxygen dependency and reactor intensification bottlenecks. Third, we apply an integral method for the direct use of time course data. The methodology is applied to four oxidative enzymes of interest: glucose oxidase, galactose oxidase, laccase and tyrosinase [4,6–8]. Besides their technological interest, these enzymes are paradigmatic cases of kinetic scenarios: high oxygen and main substrate dependency for glucose and galactose oxidase [16,35-38], high oxygen and low main substrate dependency for laccase [39] and low oxygen and low main substrate dependency for tyrosinase [40]. We show the application of the kinetic modelling for the design and anticipation of oxygen-dependent transformation in instrumented bioreactors with controlled supply of oxygen.

Materials and Methods

Materials

Glucose oxidase (GOX) from *Aspergillus niger* Type VII (G2133) with ≥100 U/mg, galactose oxidase (GalOx) from *Dactylium dendroides* (G7400) with ≥3.0 U/mg, laccase from *Agaricus bisporus* (40452)

with ≥4.0 U/mg, tyrosinase from mushroom (T3824) with ≥1.0 U/mg, peroxidase from horseradish (77332) and catalase from bovine liver (C9322) were purchased from Sigma-Aldrich (Darmstadt, Germany). All the activities are reported by the provider. Sodium di-hydrogen phosphate anhydrous was purchased from Panreac Química SLU (Barcelona, Spain), glucose monohydrate was from Merck (Darmstadt, Germany), galactose, catechol, L-tyrosine and gluconic acid were supplied by Sigma–Aldrich Chemical Co. (St. Louis, USA).

Methods

Enzyme activity assays

The activity was measured by following the initial reaction rates of oxygen consumption. Oxygen concentration was quantified using a robust oxygen micro Optical Oxygen Meter-FireStingO_2. The final reaction volume was 5 mL, containing 250 mM of glucose or galactose, 5 mM of catechol or 1 mM of L-tyrosine in 50 mM sodium phosphate buffer (NaPi) pH 7.0 and 100 µL of enzyme. 0.02 mg/mL of HRP or 0.1 mg/mL of $K_3Fe(CN)_6$ were added in the case of galactose oxidase assay to activate the enzyme. The reaction temperature was 25.0 ºC. The decrease in oxygen concentration was recorded for 5 min. One unit (U) of enzymatic activity was determined as 1 µmol of oxygen consumed per minute. Commercial enzyme powder was resuspended in 10 mM sodium phosphate at pH 7.0.

As an alternative approach, colorimetric assays can be performed. For galactose oxidase, the activity was measured by following the initial reaction rate of hydrogen peroxide using an enzyme-coupled assay. A typical enzymatic assay was performed in a Jasco FP-6300. Final reaction volume was 2 mL, containing 500 µL of 1 M galactose, 0.025 mg/mL horseradish peroxidase (HRP) and 1 mM ABTS in 50 mM sodium phosphate buffer pH 7.0 and 50 µL of enzyme. The reaction temperature was 25.0 ºC. The increase in absorbance at 420 nm was recorded for 10 min. One unit (U) of enzymatic activity was determined as 1 µmol of $ABTS^+$ produced per minute, where $\varepsilon(ABTS^+)$ =36 $mM^{-1}\cdot cm^{-1}$ and b=1 cm. For laccase, the activity was measured by following the initial reaction rate of benzoquinone formation. A typical enzymatic assay was performed in a Jasco FP-6300. Final reaction volume was 2 mL, containing 1 mM of catechol in 50 mM sodium acetate buffer pH 5.0 and 50 µL of enzyme. The reaction temperature was 25.0 ºC. The increase in absorbance at 410 nm was recorded for 10 min. One unit (U) of enzymatic activity was determined as 1 µmol of catechol consumed per minute, where ε(benzoquinone)=2,2 $mM^{-1}\cdot cm\text{-}^{1}$ and b=1 cm. For tyrosinase, the activity was measured by following the initial reaction rates of dopaquinone formation. A typical enzymatic assay was performed in a Jasco FP-6300. Final reaction volume was 2 mL, containing 500 µL of 2 mM L-tyrosine in 50 mM sodium phosphate buffer pH 7.0 and 50 µL of enzyme. The reaction temperature was 25.0 ºC. Increase in absorbance at 475 nm was recorded for 10 min. One unit (U) of enzymatic activity was determined as 1 µmol of dopachrome produced per minute, where ε(dopachrome)=3,4 $mM^{-1}\cdot cm^{-1}$ and b=1 cm.

Oxygen consumption time course measurement

Oxygen consumption time course was measured with a commercial fiber-optic oxygen sensor FireSting®-PRO (FSPRO-4) from PyroScience. The experiments were performed in a 6 mL flask controlling the temperature at 25ºC and with magnetically stirring at 250 rpm, as shown in Figure S1. The flask is not air-tight but surface aeration due to the contact of liquid surface and air on the top was checked to be negligible compared with the oxygen consumption rates. This optical oxygen sensor basically comprises two important parts: An oxygen sensitive sensor indicator and a read-out device (oxygen meter). The oxygen meter consists of a LED and photodiode which excites the oxygen sensitive indicator and detects its oxygen dependent luminescence emission. The excitation and emission light are transmitted via an optical fiber between the sensor indicator and the oxygen meter.

Study of conversion time courses in instrumented stirred tank bioreactor

Studies of complete conversion time courses were conducted in a 1 L reactor (Biostat B Plus) from Sartorius AG (Göttingen, Germany), shown in Figure S2. The reactor was equipped with a sintered metal sparger, toroidal in shape and located at the bottom of the reactor, and a Rushton turbine for mixing. Oxygen and pH were measured with probes from Hamilton Company (Bonaduz, Switzerland), specifically OXYFERM FDA 160 for oxygen and EasyFerm Plus PHI K8 160 for pH. For GOX, the reaction conditions were as follows: 500 mL of total volume, 100 mM NaPi buffer at pH 7.0, 100 mM glucose, 80 mg/L catalase, 1.5 mg/L GOX, 25 °C, 150 rpm stirring, and 50% or 25% of air saturation. For GalOx, the reaction conditions were as follows: 500 mL of total volume 50 mM NaPi buffer at pH 7.0, 20 mM galactose, 200 mg/L catalase, 50 mg/L of $K_3Fe(CN)_6$, 500 mg/L GalOx, 25 °C, 150 rpm stirring, and 50% or 20% of air saturation. At regular time intervals samples of 500 μL were withdrawn for analysis, where the reaction was stopped by pouring the sample into a vial with 450 μL of water and 50 μL of HCl 37%. Later, samples were analyzed by HPLC with a Jasco Plus HPLC equipped with Benson polymeric (BP-800 H^+) carbohydrate column at 60 ºC. A solvent mixture of H_2O and H_2SO_4 0.005 M was employed as the mobile phase with a flow rate of 0.5 mL/min. For the analysis of gluconic acid, the absorbance at 218 nm was followed within 15 min with a multiwavelength MD-2015 Jasco Plus detector and for the analysis of galactose, the refractive index was followed within 15 min with a RI-2031 Jasco Plus detector. Linear standard curves for gluconic acid and galactose were obtained, with a regression coefficient of 0.9994 and 0.9954, respectively.

Theoretical framework of kinetic analysis

The expression of the specific reaction rate given by a certain amount of enzyme (Activity: *Act*) is given by Eq 1. The ratio (γ) between the enzyme activity (*Act*) and the maximum enzyme activity (Act_{max}) can be expressed only as a function of $[O_2]$, K_{O2} and S/K_s as shown in Eq 2.

$$\gamma = \frac{[S]\cdot[O_2]}{[S]\cdot[O_2]+K_S\cdot[O_2]+K_{O_2}\cdot[S]} \quad \textbf{Eq 2}$$

When the oxygen concentration is constant, Eq 1 is simplified to an apparent MM kinetics depending on *[S]*:

$$R = \frac{Act_{maxapp}\cdot[S]}{K_{Sapp}+[S]} \quad \textbf{Eq 3}$$

K_{Sapp} is the apparent constant for the substrate, defined as:

$$Ks_{app} = \frac{K_S\,[O_2]}{K_{O2}+[O_2]} = K_S\,O_2^* \quad \textbf{Eq 4}$$

Act_{maxapp} is the maximum activity observable at fixed oxygen concentration:

$$Act_{maxapp} = \frac{Act_{max}\,[O_2]}{K_{O2}+[O_2]} = Act_{max}\,O_2^* \quad \textbf{Eq 5}$$

When the substrate concentration is constant, Eq 1 is simplified to an apparent MM kinetics depending on $[O_2]$:

$$R = \frac{Act_{maxapp}\cdot[O_2]}{K_{O2app}+[O_2]} \quad \textbf{Eq 6}$$

K_{O2app} is the apparent constant for the oxygen, defined as:

$$K_{O2app} = \frac{K_{O2}\,[S]}{K_S+[S]} \quad \textbf{Eq 7}$$

$Act_{O2maxapp}$ is the maximum activity observable at fixed S concentration:

$$Act_{maxapp} = \frac{Act_{max}\,[S]}{K_S+[S]} \quad \textbf{Eq 8}$$

Elucidation of the kinetic model based on the differential calculation method

The differential method from the point of view of *[S]* or $[O_2]$ was performed in OriginPro 2019. In this software, activity (y axis) vs concentration of substrate (x axis) is required as input. In the case of *[S]* variation, initial oxygen consumption rates were calculated. In the case of $[O_2]$ variation, it was necessary to perform a graphical differentiation through finite increments of the integral data (oxygen-time). To make this differentiation, a specific time interval is chosen and the mean of the concentration in that interval is used. Typically, the time increment chosen for graphic differentiation was 5-10 seconds. Then, a non-linear curve fit of the activity vs oxygen concentration data is carried out. Among all the different non-linear fittings, enzyme kinetics functions are included, and specifically the Michaelis-Menten hyperbolic function was chosen to fit the experiments. The output of the fitting report shows the Act_{max} and K_m parameters (Equations 3 and 6) of the model together with the statistical

parameter R^2, which is the proportion of the variance in the dependent variable that is predictable from the independent variable.

Elucidation of kinetic model based on the integral calculation method

Integration of Eq1 by single response fitting was performed in Berkeley Madonna software using a combination of Rosenbrock(stiff) method for the integration with a Levenberg-Marquardt algorithm for the non-linear regression. Berkeley Madonna is a mathematical modelling software package which numerically solves ordinary differential equations and difference equations. $[O_2]$ vs time experiments were imported to the software and then the option "Curve fit" was used to fit the simulated data of every oxygen time course case-by case to the experimental data according to Eq 1. The software fits the experiments by finding the minimal SQR. To impose restrictions, the information from the differential model was used (K_{Sapp} was fixed), and the Act_{max} and K_{O2} were obtained from the fitting, together with the statistical parameter RMSE given by the software.

Integration of Eq1 by multiple response fitting was performed in Aspen Custom Modeler software v11, namely by combining an Implicit Euler method with variable step for the integration of the differential equation with the NL2SOL adaptative non-linear regression algorithm. Aspen Custom Modeler v11 is specifically designed for development and use of custom process models. O_2 vs time experiments were imported to the software and then the option "Estimation Parameters" was used to fit simultaneously all the simulated data of the oxygen time course to the experimental data according to Eq 1. The software fits the experiments by finding the minimal SQR. To impose restrictions and assist the model to fit the data, the Act_{max} from the differential method was fixed and the K_S and K_{O2} were obtained from the fitting in case of the GOX and GalOx. For the laccase and tyrosinase the K_S from the single response analysis was fixed, and the Act_{max} and K_{O2} were obtained.

As quantification of the goodness of the kinetic constant calculation, different parameters were shown. The squared error of estimates (SQR) is the sum of variance for the whole set of data. Other goodness-of-fit parameters can be derived from SQR including the degrees of freedom, that is, the difference between the number of data and the number of kinetic parameters: Fisher's F parameter (the higher its value, the better, with ∞ as the best value), the root of mean squared errors (RMSE) (the lower, the better, with zero as the ideal value) and information criteria directly created for mathematical model selection; being the Akaike criterion (AIC) the original one (the lowest its value, the better the fitting, with -∞ as the best value).

RESULTS AND DISCUSSION

Measurable activity effectiveness in the use of the enzyme: implications for process implementation

Although it is well known that the measurable activity of an oxidase depends on both concentration of oxygen and main substrate concentration, the interdependence of the apparent kinetic constants and its importance for process implementation is by far less understood. The application of classic principles of chemical reaction engineering enabled by the development of new analytical technologies gives a fresh perspective. Setting conditions of air saturation ($[O_2]$ = 0.25 mM), the ratio of reaction velocity (measurable activity) given by an oxidase compared to the maximum, γ , can be expressed only as a function of S, K_S and K_{O2}, Eq 2. Figure 1 shows cases for a low and high value of K_S. In cases of enzymes with a low saturation constant for S (K_S<1mM), there is a wide range of substrate concentration to operate at maximum apparent velocity, Figure 1A. For situations where the saturation constant of the substrate is high (e.g. K_S>10mM), Figure 1B, this region of operation at maximum velocity decreases. The effectiveness, γ, however is only limited by the intrinsic saturation constant for the oxygen, K_{O2}, the values reached of γ are higher when K_{O2} is lower. In Figures 1A and 1B the areas where there is no limitation of the main substrate have been shaded, in that area the enzyme operates at constant velocity saturated by the main substrate only limited by the intrinsic kinetics toward O_2. The unshaded area corresponds to the region where there is also limitation by the main substrate. These graphs can be merged in a unique graph, Figure 1C, where γ is expressed in function of the normalized concentration of substrate ($[S]/K_S$) at different K_{O2}, following equation 9:

$$\gamma = \frac{\frac{[S]}{K_S}\cdot\frac{[O_2]}{[O_2]+K_{O_2}}}{\frac{[S]}{K_S}+\frac{[O_2]}{[O_2]+K_{O_2}}} = \frac{S' O_2^*}{S'+O_2^*} \qquad \textbf{Eq 9}$$

Where the term $\frac{[O_2]}{[O_2]+K_{O_2}}$ expresses the O_2 limitation (O_2*) and S' expresses the normalized concentration of substrate ($[S]/K_S$), the expression γ is a rectangular hyperbola with a maximum value equal to O_2*, the normalized concentration of substrate needed to achieve half of O_2* is also O_2*. The value of the effectiveness γ depends on the intrinsic kinetics towards oxygen, whereas the window for constant maximum velocity depends on the saturation constant for the oxygen and of the K_S. Maximization of the use of the enzyme and the reactor productivity needs the calculation of these values. Figure 1D illustrates the consequences of γ in a representative conversion course of an oxidase. Operation time is normalized to dimensionless time ($time \cdot Vmax/[S]_{initial}$).

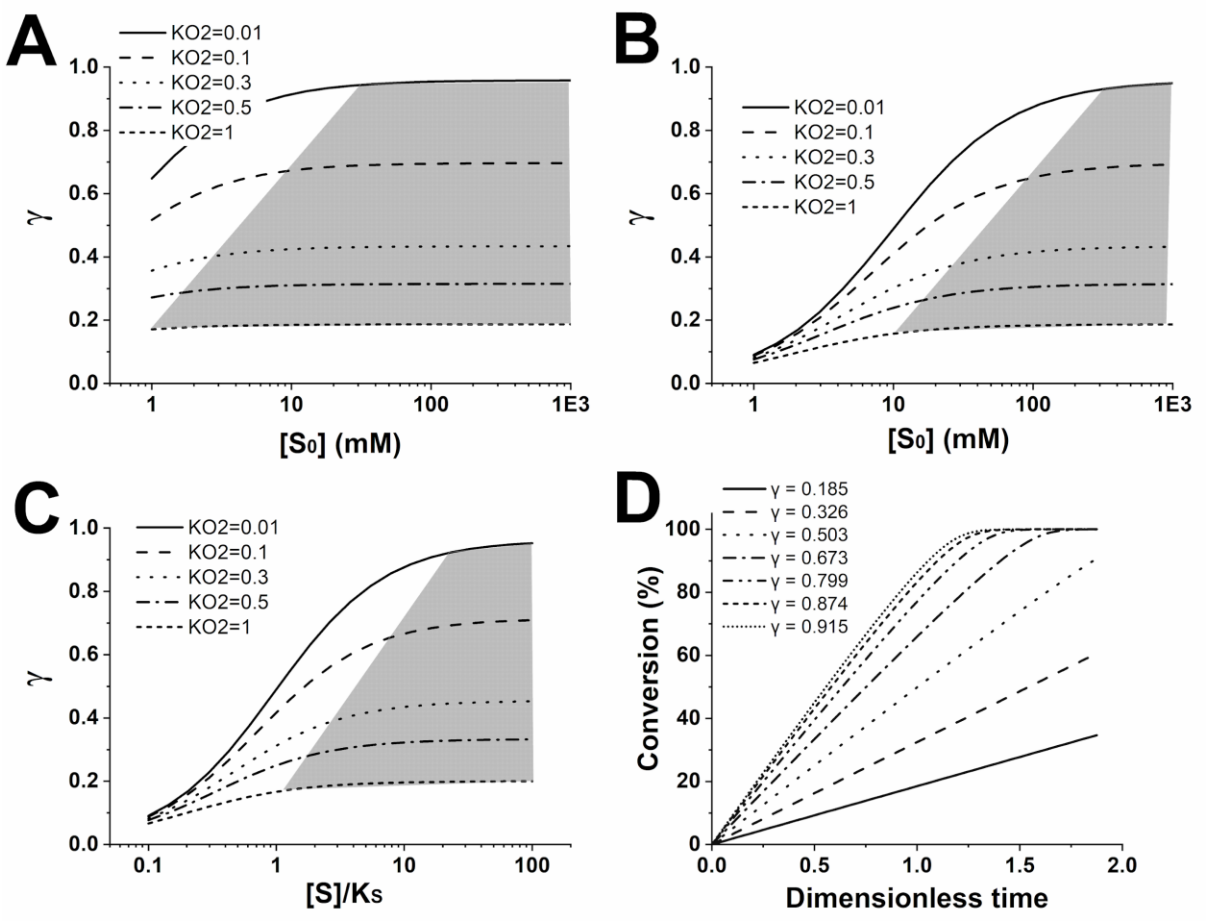

Figure 1. Panel A: Ratio of measurable activity to maximum activity, γ, as function of the substrate concentration, *[S]*, varying K_{O2} (mM), *Ks*=0.5 mM; Panel B: Ratio of measurable activity to maximum activity, γ, as function of the substrate concentration, *[S]*, varying K_{O2} (mM), *Ks*=10 mM; Panel C: Ratio of measurable activity to maximum activity, *γ*, in function of the normalized concentration of substrate (S/K_S) at different K_{O2} (mM); Panel D: Conversion of the main substrate *[S]* vs dimensionless time for different values of *γ*, S_0/K_S=20. $[O_2]$=0.25 mM, *[E]*=0.1 mg/mL, Act_{max}=5 U/mg.

The analysis of operational limitations regime emphasizes the importance of the identification of the saturation constants at an early stage of catalyst development. Calculation of K_{O2} is crucial for the identification of the oxygen limitations, whereas the calculation of K_S is essential to locate the concentration of substrate needed to reach full velocity, which will be eventually limited by the main substrate solubility. A systematic analysis could be performed by systematic variation of *[S]* at fixed $[O_2]$ and systematic variation of $[O_2]$ at fixed *[S]*. However experimental approaches for variation of initial $[O_2]$ require sophisticated equipment. Another possibility is a combination of the differential and integral analysis based on oxygen time conversion courses. This is developed and shown as follows.

Differential analysis to elucidate main substrate dependency.

The activity of an oxidase can be quantified by following the initial reaction rate of oxygen consumption or product formation, $\frac{dO_2}{dt}|_{t\to 0}$, according to Eq 1. By measuring the activity at different initial *[S]* at fixed concentration of oxygen the Act_{maxapp} and the K_{Sapp}, both including by O_2^*, can be calculated according to Eq. 3-5. Figure 2 shows the Act/[S] plot for different oxidases. GOX and GalOx show medium-high values of K_{Sapp} whereas tyrosinase and laccase show low values of K_{Sapp}.

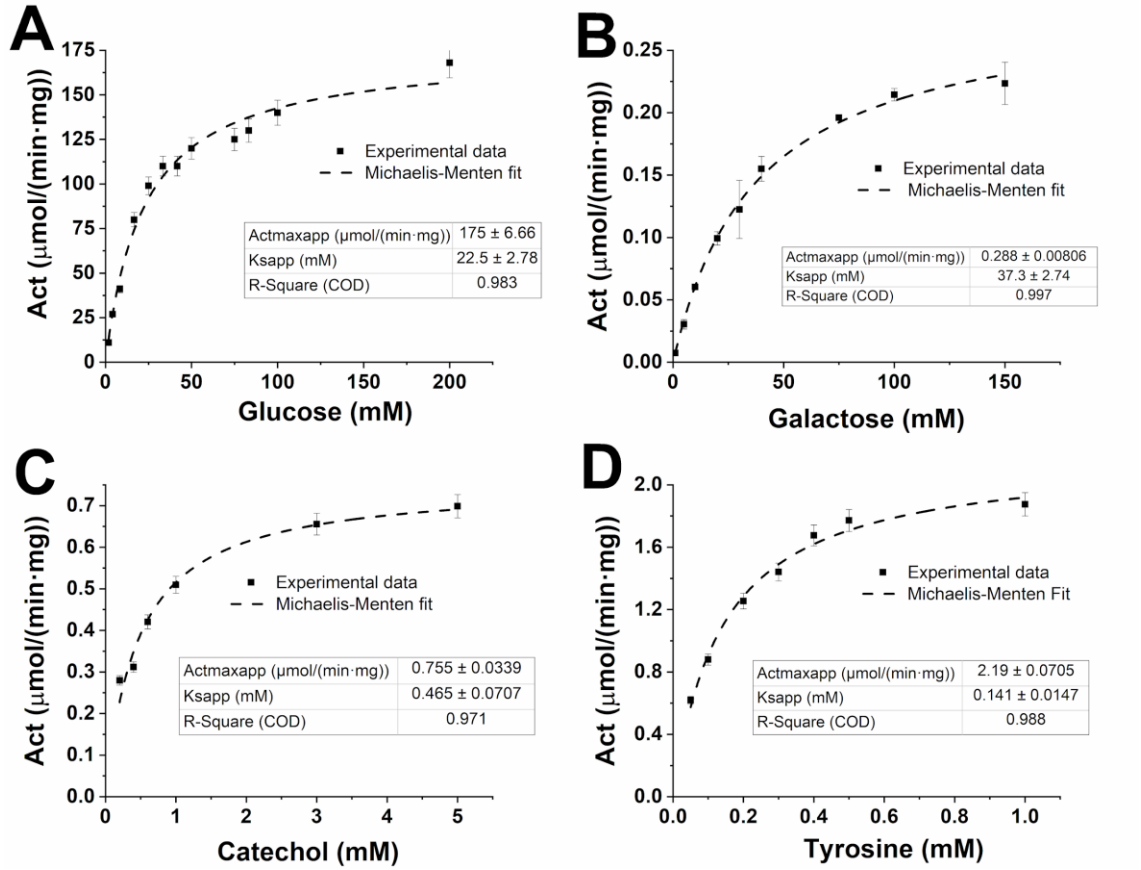

Figure 2. Plots of activity vs *[S]* for different enzymes, with K_{Sapp} calculated according to Eq. Experiments were performed at 25ºC in 50 mM sodium phosphate buffer pH 7.0. Panel A: GOX, Panel B: GalOx, Panel C: laccase, Panel D: tyrosinase.

From the experiments performed, it would be possible to simulate the performance of the enzyme catalyzed reaction when full air saturation is used, but the intrinsic K_{O2} cannot be calculated, and it is not possible to predict the consequences of different level of air saturation on the performance of the enzyme catalyst. The calculation of activity based on initial consumption rates is affected also by some uncertainty given the high oxygen dependency (linear phase is hardly capturable as shown below). Additionally, the intrinsic value of *Ks* and localization of operational regime of the enzymes remains also unknown. However, it is possible to restrict the values. Once K_{Sapp} is defined, a locus is described by the combinations of K_S and K_{O2} that are consistent with K_{Sapp} (Eq 10). The result is shown in Figure 3, there is a proportional dependence between K_S and K_{O2}, in other words, with the sole information of K_{sapp}, situations of both high oxygen and substrate dependency are hardly disentangled. However, it is

possible to situate the order of magnitude, very useful to anticipate the influence of *[S]*. Figure 3A shows the locus for GOX and GalOx, with potential values of K_S of hundredfold, whereas Figure 3B shows the locus for tyrosinase and laccase, with low values of K_S. Relationship of Eq 10, illustrated in Figure 3, will be used in the following sections for quantitative analysis.

$$Ks = Ks_{app} + Ks_{app} \frac{KO_2}{O_2} \qquad \textbf{Eq 10}$$

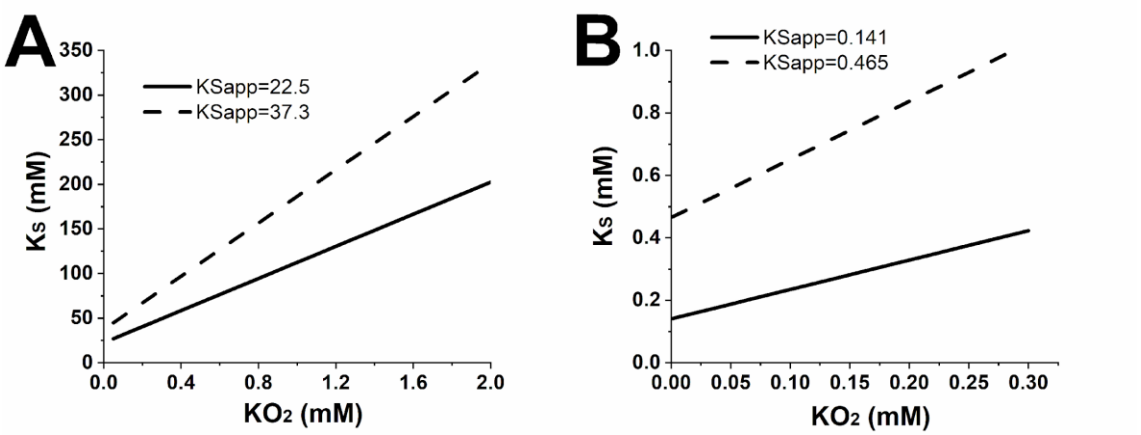

Figure 3. Different pairs of combinations of K_S and K_{O2} that satisfy the calculated K_{Sapp} values calculated according Eq 10. Panel A is for GOX (continuous line) and GalOx (dashed line) while Panel B is for laccase (dashed line) and tyrosinase (continuous line). $[O_2]$= 0.25 mM.

Differential analysis to elucidate O_2-dependency.

The analysis of the oxygen dependency can be only elucidated by observation of rate upon O_2 variation. Setting and controlling an oxygen concentration different from air saturation is generally based on specialized reactor setups as described in introduction [13-18,23,28]. To simplify and allow a generally applicable approach working under fixed air saturation, we make use of the widespread new sensing technologies and the physicochemical features of the oxidation reactions. Currently optochemical sensing offers the possibility to quantify the oxygen consumption in conventional bench-lab set-up with high precision and short time response. Under the condition of $[S]>>[O_2]$, $[S]$ can be assumed as constant, and the monitoring of the full dissolved oxygen time conversion course is very useful to analyze the kinetics based on Eq. 6. Figure 4 shows an illustrative set of observations dependent on the intrinsic kinetic.

Figure 4 illustrates different scenarios located in the space defined by the following vertices: (K_{O2} low, K_S low), (K_{O2} low, K_S high), (K_{O2} high, K_S low), (K_{O2} high, K_S high). Panels A and B illustrate what to expect in vertices of S/K_S depending on the intrinsic kinetics towards O_2. At a high level of O_2

dependency (K_{O2} high) lines become more curved showing the decrease of the reaction rate upon reaction progress, at low level of O_2 dependency (K_{O2} low), lines are straight manifesting the zero-reaction order toward oxygen. Panels C and D give the perspective from systematic variation of substrate concentration for a fixed enzyme under two K_{O2} vertices. In case of low level of O_2 dependency (K_{O2} low; Panel C), the whole set of reaction curves are straight independent on the saturation with *S*. For the cases of high level of O_2 dependency (K_{O2} high, Panel D), lines are curved and only become straight when substrate is limiting. Hence identification of curved lines is an evidence of O_2 limitation in the range of oxygen solubility, whereas straight lines might manifest absence of O_2 limitation or counterintuitively limitations of both substrates (K_S high/K_{O2app} low according Eq 7).

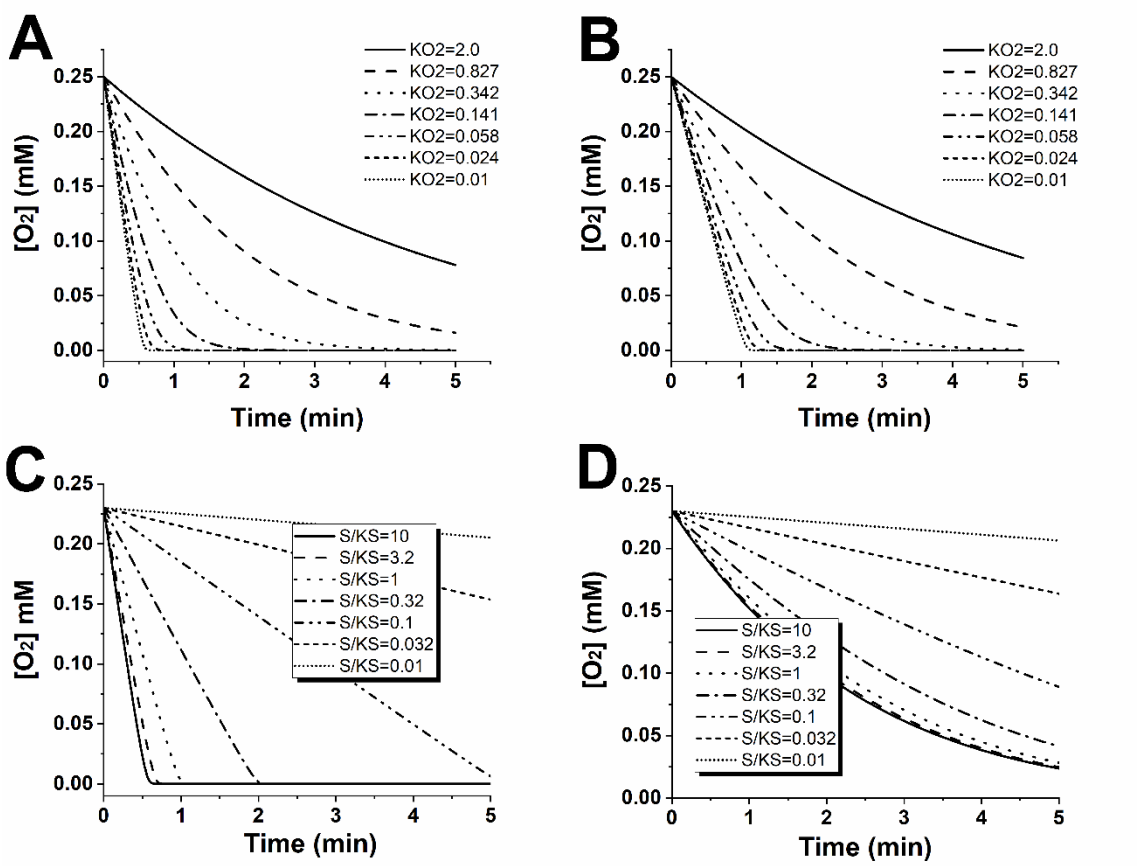

Figure 4. O_2 time courses at different values of K_{O2} (mM) and $[S]/K_S$. Panel A, K_S=0.1 mM; Panel B, K_S=100 mM; Panel C, K_{O2}=0,01 mM; Panel D, K_{O2}=1 mM. $[S_0]$=100 mM, $[E]$=0.1 mg/mL, Act_{max}=5 U/mg.

A more insightful perspective on the kinetic equation can be obtained by acquiring the first derivative of the concentration vs time curve. By graphical differentiation of the data from Figure 4, we can obtain the data of activity vs O_2. For this plot it is possible to evaluate K_{O2app}. K_{O2app} depends on $[S]$, K_{O2} and K_S according to Eq 7. Illustrative results are shown in Figure 5.

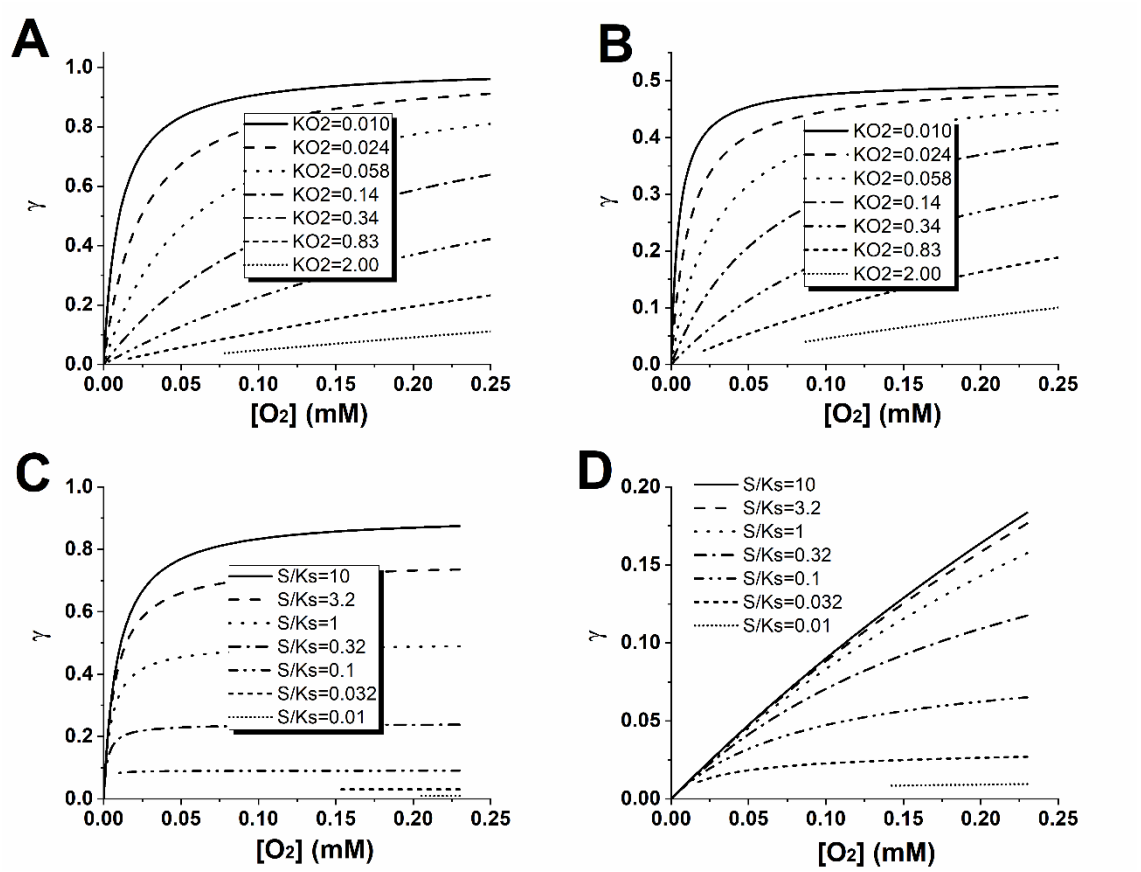

Figure 5. Ratio of measurable activity to maximum activity, γ, vs O_2 at different values K_{O2} (mM) and *S/Ks*. Panel A, K_S=0.1 mM; Panel B, K_S=100 mM; Panel C, K_{O2}=0,01 mM; Panel D, K_{O2}=1 mM. Conditions common to all panels: $[S_0]$=100 mM, *[E]*=0.1 mg/mL, Act_{max}=5 U/mg.

Panels A and B illustrate what to expect in extreme situations of $[S]/K_S$ depending on the intrinsic kinetics towards O_2. In both cases, at high levels of O_2 dependency (K_{O2} high) lines become straighter showing the O_2 control (first order reaction) and nearly proportional increase of the reaction rate upon increase of O_2. At low level of O_2 dependency (K_{O2} low), lines are curved showing a clear rectangular hyperbolic shape manifesting the achievement zero-reaction order toward oxygen at high O_2. Panels C and D give the perspective from systematic variation of substrate concentration for a given enzyme under two extreme scenarios. In case of low level of O_2 dependency (K_{O2} low), the whole set of lines are hyperbolic with a constant maximum reaction rate achieved at a certain level of O_2. The lowest the $[S]/K_S$, the largest is the zone with zero-order dependency, the lowest the K_{O2app}. For the cases of high levels of O_2 dependency (K_{O2} high), lines are straight and only become hyperbolic manifested in more horizontal lines when substrate is limiting, which promotes a decrease of K_{O2app}. Hence identification of straight lines is an evidence of O_2 limitation in the range of oxygen solubility, whereas curved lines that become horizontal might manifest absence of O_2 limitation or counterintuitively limitations of both substrates. The change of curvature in Panels C and D is related to the change of the apparent K_{O2app}, which can be calculated from the previous graphs by application of suitable calculation methods. An

extreme situation occurs when the K_{O2app} equals the intrinsic K_{O2}, (for very high $[S]/K_S$) and therefore it can be obtained directly, this is only feasible when K_{O2} is significantly lower than the initial $[O_2]$. These were applied as follows for the study cases.

Based on this analysis framework, dissolved oxygen consumption time courses were measured upon variation of substrate concentration (Figure S3-S7). The amount of enzyme, *[E]*, was sensibly managed to access enough number of data points both at low and high level of air saturation. Figure 6 shows the result of the graphical differentiation of oxygen time courses. Panels A and B show the result for the GalOx and GOX, which resemble the result of Figure 5D. Panel A shows mainly straight lines in a broad range of oxygen, lines are only slightly curved getting saturation at very low concentration of *S*. In both cases, but especially in the GOX, it is possible to observe how the line of act diverges extremely at high O_2, indicating a high oxygen dependency, but they are a converging bundle of straight lines at low O_2, indicating first order at low O_2. Panels C and D shows the result of the laccase and tyrosinase. Panel C shows a more similar case to panel 5C, in which the lines are more curved, still it was difficult to capture apparent oxygen saturation due to the difficulty to decrease S without compromising the imposed stoichiometric limitation of oxygen. Panel D shows curve activity plots indicating the approach to saturation with oxygen in the range of solubility, quite like Figure 5C.

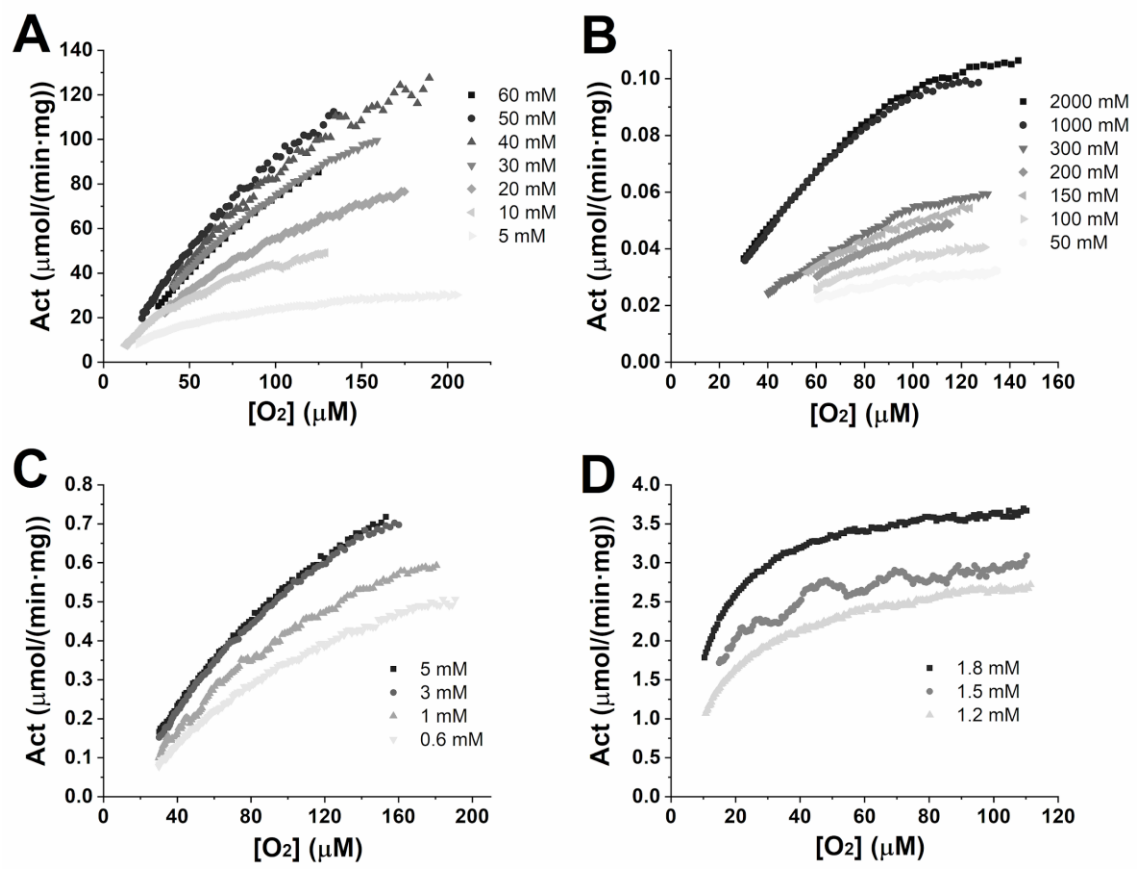

Figure 6. Activity vs oxygen concentration data obtained from the differentiation of the integral data (oxygen vs time) for each enzyme. Panel A: Activity (µmol/(min·mg)) vs [O_2] (µM) for GOX, Panel B: Activity (µmol/(min·mg)) vs [O_2] (µM) for GalOx, Panel C: Activity (µmol/(min·mg)) vs [O_2] (µM) for laccase, Panel D: Activity (µmol/(min·mg)) vs [O_2] (µM) for tyrosinase.

Once we analyze qualitatively all data, we aim to establish a suitable kinetic modelling. Data are analyzed based on the Eq 6, where a K_{O2app} can be calculated. Figure 7 shows the results for the three first enzymes, while Table 1 shows the results for the tyrosinase. For GOX, K_{O2app} is easily calculated for the range of glucose 60-5 mM based on Eq. 6, whereas a first order potential model would work better for *[Glucose]* > 60 mM, since K_{O2app} increases upon *[S]* and apparent saturation with $[O_2]$ is not possible under air saturation. This is an indication that the intrinsic K_{O2} lies above the value of air saturation. From the dependency of K_{O2app} vs glucose, and using Eq 7, K_{O2} and K_S can be calculated, and from the dependency of Act_{maxapp} vs glucose, and using Eq 8, K_S and Act_{max} can be calculated, as shown in Table 2. For GalOx and laccase, panel C and E show the dependency of K_{O2app} approaching a value for K_{O2} at high substrate concentrations which can be calculated using Eq 7, and the value of K_S can be calculated according to Eq 8, as shown in panels D and F, respectively. Figure S8 shows the result when $K_3Fe(CN)_6$ is used as an activator. For tyrosinase, given the low value of the intrinsic K_S and therefore the very high value of $[S]/K_S$ achievable under the value of substrates used, all the values of K_{O2app} approach the intrinsic value K_{O2}, shown in Table 1. The results of estimation of the intrinsic constant are shown in Table 2. As expected from the analysis shown in Figure 3, GOX and GalOx display hundredfold values of Ks, whereas laccase and tyrosinase display lower values. For reaction intensification focused on substrate feeding, both *[S]* and $[S]/K_S$ are important. The initial *[S]*, which depends on solubility, determines the maximum achievable product concentration whereas $[S]/K_S$ determines the kinetic regime (as shown in Figure 1). A further analysis of reaction intensification requires, therefore, the joint application of kinetic analysis and reaction medium engineering.

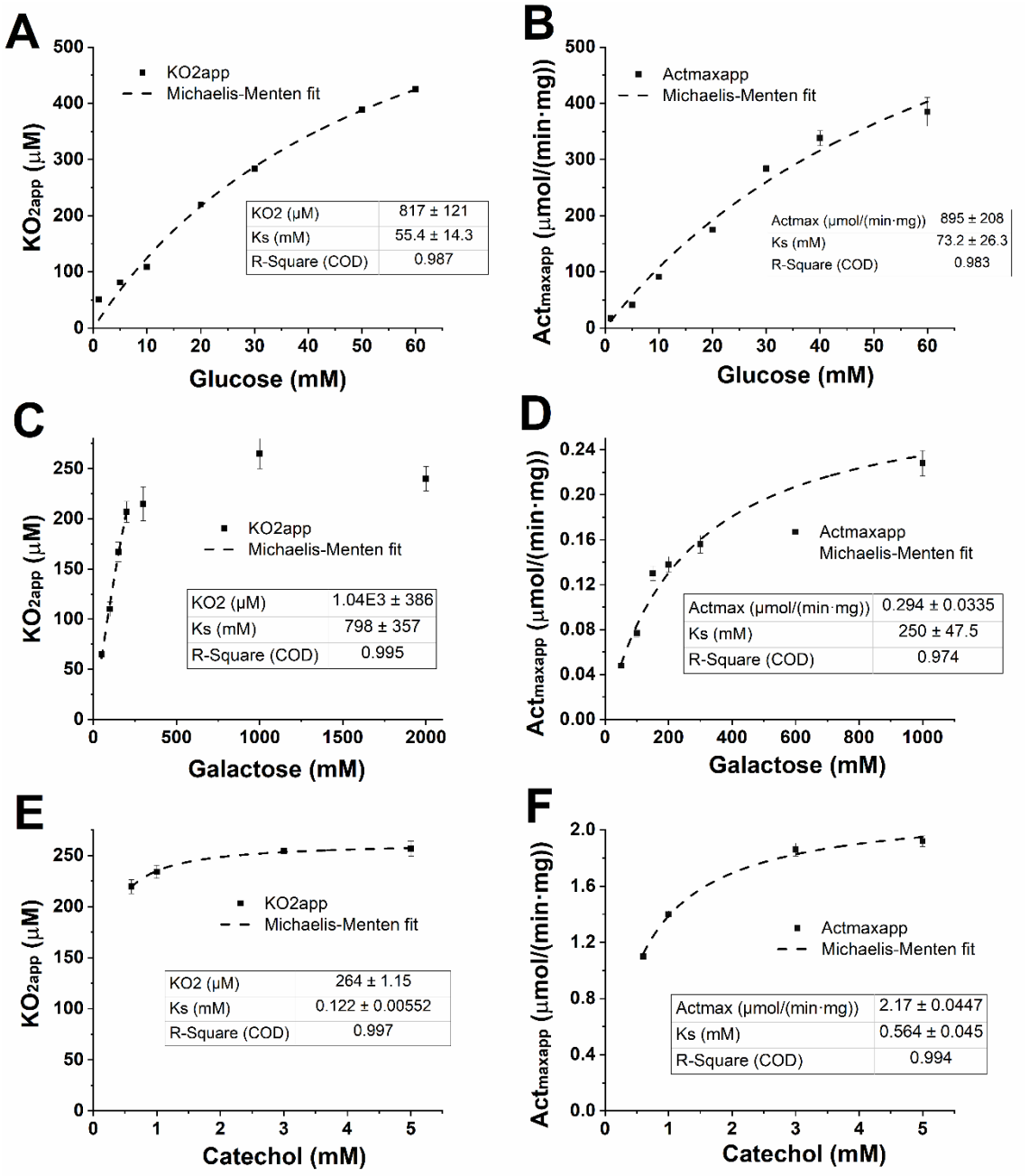

Figure 7. Differential analysis of the oxygen-dependent apparent kinetic parameters versus the main substrate [S] for GOX, GalOx and laccase. Panel A: K_{O2app} *vs [S]* for GOX, Panel B: Act_{maxapp} *vs [S]* for GOX, $[E_{GOX}]$= 0.0015 mg/mL; Panel C: K_{O2app} *vs [S]* for GalOx, Panel D: Act_{maxapp} *vs [S]* for GalOx, $[E_{GalOx}]$= 1 mg/mL; Panel E: K_{O2app} vs *[S]* for laccase, Panel F: Act_{maxapp} *vs [S]* for laccase, $[E_{Laccase}]$= 0.8 mg/mL.

It is worth highlighting a particularity in Figure 7C. High concentration spots have been discarded as they have been misinterpreted in the non-linear regression. When performing the GalOx reaction with HRP as activator, a latency phase is detected at the beginning of the reaction (Figure S4), characterized with a transition from a convex curve to the usual concave curve, which creates a false local maximum of activity (Figure S4) that the software has interpreted as having reached oxygen saturation (K_{O2app}

close to 250 μM), but really the value of the constant is close to 1200 μM as shown in Figure S8 with the other activator. On the other hand, for laccase in Figure E only the saturation points of the hyperbola have been captured, as well as in Table 1 only saturation values of K_{O2app} for tyrosinase are shown. The problem is that when working at concentrations of the main substrate with close values of saturation with air, it also begins to limit the main substrate, the reaction speed decreases a lot and values close to zero of oxygen concentration are not reached, therefore it is not possible to undertake the fitting to Eq 6. Additionally, the management of differential data requires the differentiation of oxygen time courses which is associated with the increase of propagation errors. This affects the measurement of the activity based on initial reaction rates and certainty of calculation of act vs concentration plots. In the following section, we show how to interpret and calculate kinetic constants by directly using the integral data.

Table 1. Values of K_{O2app} and Act_{maxapp} for tyrosinase obtained from the differential analysis of the oxygen-dependent apparent kinetic parameters versus the main substrate *[S]*. $[E_{Tyrosinase}]$ = 0.5 mg/mL.

Tyrosine (mM)	K_{O2app} (μM)	$Act_{max\ app}$ (μmol/(min·mg))
1.8	11.6	4.07
1.5	13.3	3.32
1.2	19	3.15

Table 2. Values of the parameters obtained from the differential analysis for each enzyme, with the statistical analysis.

	GOX	GalOx_HRP	GalOx_ $K_3Fe(CN)_6$	Laccase	Tyrosinase
K_{Sapp} *(mM)*	22.5 ± 2.78	32.9 ± 4.03	37.3 ± 2.74	0.465 ± 0.071	0.141 ± 0.015
K_{O2} *(μM)*	817 ± 121	1250 ± 238	1202 ± 267	264 ± 1.15	11.6 ± 0.58
K_S *(mM)*	55.4 ± 14.3	250 ± 47.5	241 ± 53.5	1.05 ± 0.046	0.147 ± 0.050
Act_{max} *(μmol/(min·mg))*	895 ± 208	0.294 ± 0.033	2.33 ± 0.55	2.17 ± 0.045	4.07 ± 0.010
SQR	249	1812	888	3015	615
RMSE	1.44	3.11	2.94	15.7	4.4
F Fischer	32511	3811	4492	53284	63074
AIC	46	281	157	207	357

How to elucidate intrinsic O_2 kinetics: integral analysis

Direct use of oxygen time courses was carried out for kinetic analysis. Qualitative inspection of time courses as shown in Figure 4 is very useful to situate the significant range of the kinetic constants. For quantification, an integral simple response analysis is then performed with Berkeley Madonna software. Each oxygen time course was fitted independently for the calculation of constants. Figures S10-S14 show all the fittings. It should be remembered that when using integral data, performing an integral

method to estimate parameters leads to more exact values than using differential methods, because in this way the error is avoided when differentiating. For this, the oxygen-time data are adjusted to the proposed Ping-Pong model by minimizing residuals squared. An example of the fittings made is shown in Figure 8. Table 3 (full set can be found in Table S1-S11) shows the kinetic parameters obtained for the kinetic model and the relevant statistical parameters of the fit. Constraints of Figure 3 (Equation 10) were used to assist the fitting and involving the *S* dependency. Values from differential analysis were used as initial guesses. Results show how the application of one step of fitting reached values in agreement with the analysis previously performed, Table 3, but with better values of fitting goodness parameters (F, AIC).

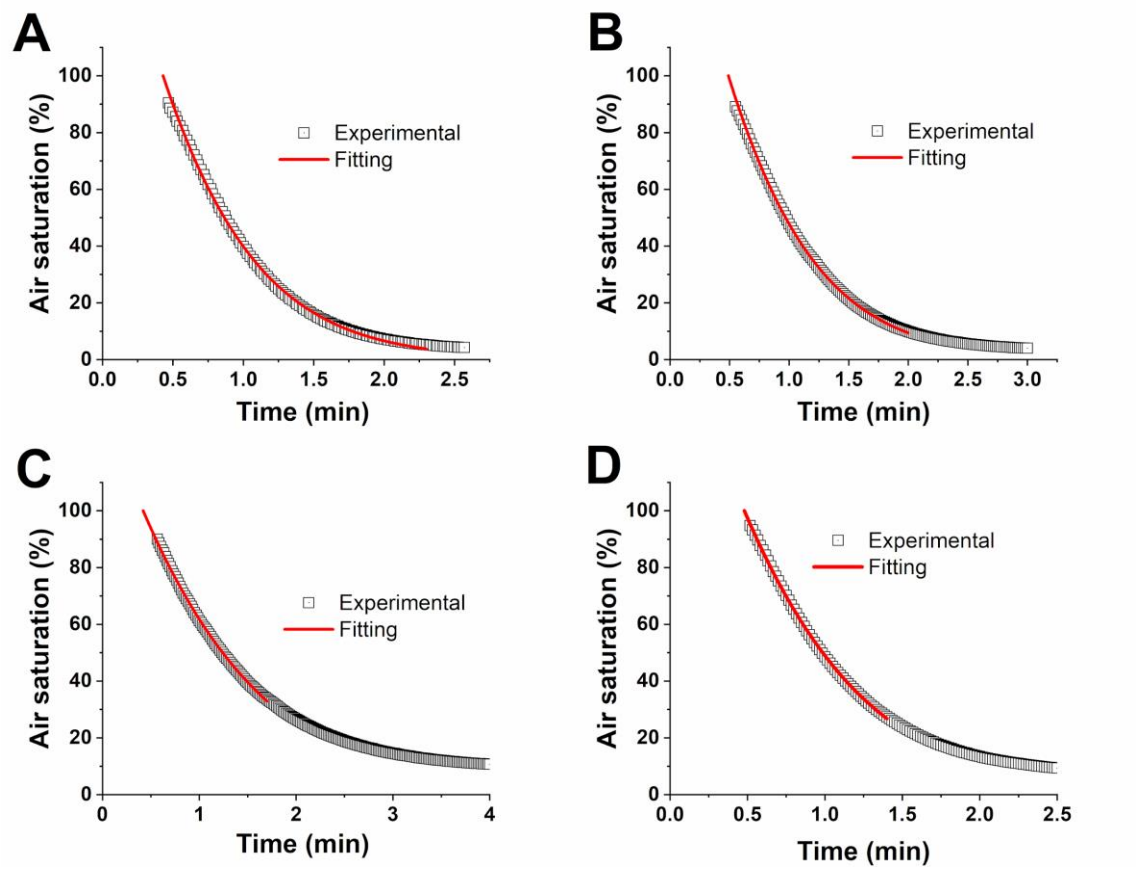

Figure 8. Single response analysis fitting performed in BM for the GOX. Panel A: 2000 mM glucose, Panel B: 400 mM glucose, Panel C: 200 mM glucose, Panel D: 100 mM glucose.

Table 3. Values of the parameters obtained from the integral analysis single response for each enzyme, with the statistical analysis.

	GOX	**GalOx_HRP**	**GalOx_KCNFe$_3$**	**Laccase**	**Tyrosinase**
K_{O2} (μM)	785 ± 122	1640 ± 175	1680 ± 184	348 ± 52.0	14.0 ± 3.6
K_S (mM)	105 ± 15.8	287 ± 29.5	323 ± 41.7	1.22 ± 0.18	0.149 ± 0.016
Act_{max} (μmol/(min·mg))	740 ± 91.7	0.272 ± 0.103	3.062 ± 0.559	2.35 ± 0.49	4.12 ± 0.304
SRC	103	89	31	13.1	124
RMSE	0.71	0.70	0.59	0.292	0.48
F Fischer	1231341	984556	308094	2208066	4274416
AICc	-202	-180	-84.7	-357	-598

Next, the integral multiple response analysis is performed with Aspen Custom Modeller software. All the oxygen time courses upon variation of initial substrate concentration were simultaneously used and restriction from Figure 3 (Equation 10) was not applied. In this case, two independent variables are included at the same time in the fitting, introducing cross effects of these variables and leading to even more precise values of the parameters to be estimated. To do this, the oxygen-time data are adjusted to the proposed Ping-Pong model by minimizing residuals squared. An example of the adjustments made is shown in Figure 9, full set of fitting are shown in Figure S15-S18. Table 4 (Table S12-S17) shows the parameters obtained from the fitting. Values of fitting goodness parameters (*F, AIC*) were further enhanced.

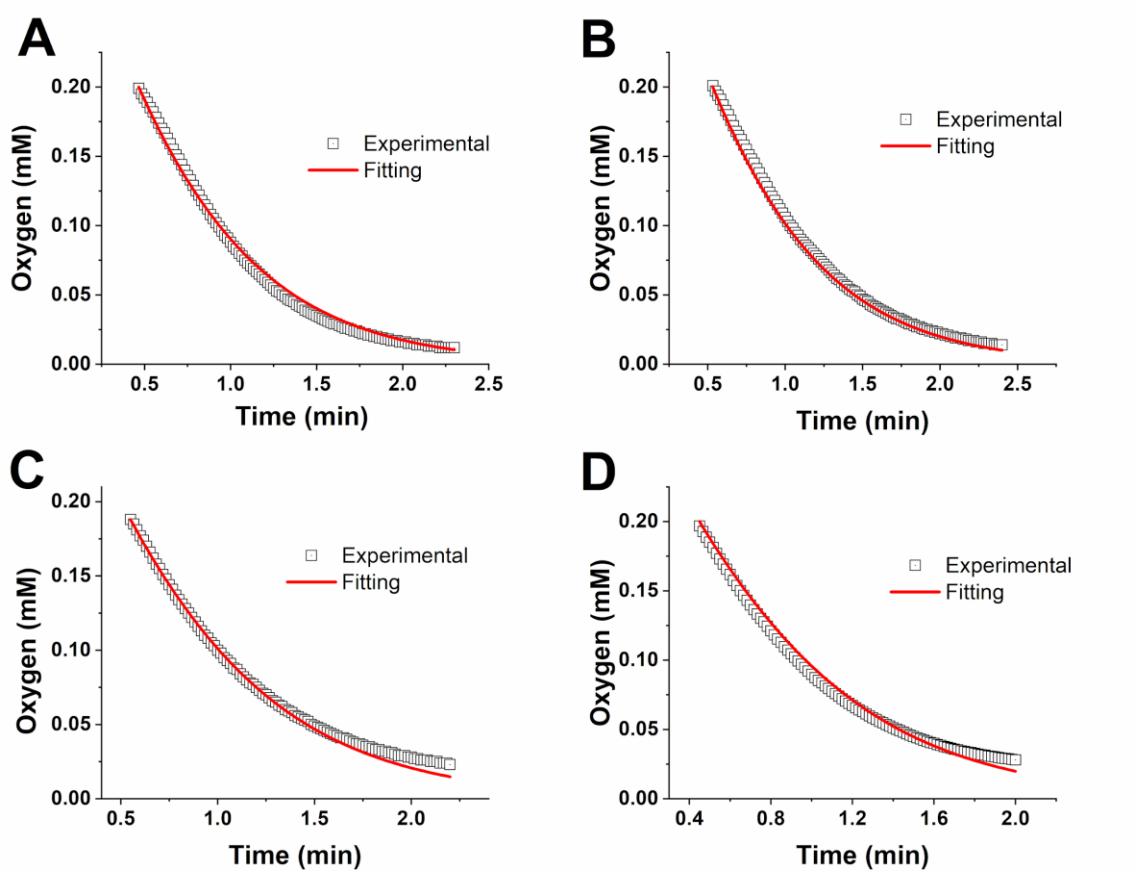

Figure 9. Multiple response analysis fitting performed in Aspen for the GOX. Panel A: 2000 mM glucose, Panel B: 400 mM glucose, Panel C: 100 mM glucose, Panel D: 75 mM glucose.

It is interesting to note the lack of end-time adjustment in some cases. This can be due to two factors. The first, phenomenological, consists of a lower oxygen consumption rate than expected, probably due the difficulties to reach anoxia levels in not hermetic reactor set-ups or deeper features of the kinetic mechanism. The second factor is specific to the adjustment mechanism. The software tends to better adjust the data from the beginning because it has a higher specific weight, that is, the squared residuals of the values at higher concentrations are higher and therefore the software minimizes them more. The choice of the amount of enzyme used (and profile of the O_2-time obtained) should be therefore adapted depending on the relevant region for the significance of the intrinsic constants.

Table 4. Values of the parameters obtained from the integral analysis multiple response for each enzyme.

	GOX	**GalOx**	**Laccase**	**Tyrosinase**
K_{O2} **(μM)**	741 ± 3.0	2070 ± 18.0	305 ± 9.0	16.0 ± 1.47
K_S **(mM)**	53.3 ± 1.5	460 ± 7.7	1.22 ± 0.18	0.150 ± 0.002
Act_{max} **(μmol/(min·mg))**	740 ± 91.7	3.06 ± 0.56	1.10 ± 0.01	5.43 ± 0.064
SRC	0.0702	0.161	0.00599	4.04
RMSE	0.0246	0.0360	0.00582	0.099
F Fischer	15625	151947	1624768	23822269
AICc	-775	-667	-1415	-1878

Once the parameters of the model are calculated, we can compare them with the parameters available in the literature. For the GOX, Ringborg and co-workers [16] investigated the oxidation of glucose at 25ºC in tube-in-tube flow reactor, where the oxygen concentration was varied from 0.2 to 7 mM, and they reported a K_S of 75±9.4 mM and a K_{O2} of 520±9.0 μM. The very slight differences can be due to the type of reactor used and the higher oxygen concentrations employed in the tube-in-tube reactor. This complex configuration allows reaching a higher concentration of oxygen, and, therefore, it enables a fine-tuned calculation of the high K_{O2}, whereas our configuration is much simpler and easier to implement but requires numerous experiments and careful calculation work. However, a step-by-step careful calculation process renders similar values for both parameters. Regarding the GalOx, Kwiatkowski and co-workers [35] analyzed the oxidation of galactose at 20°C with GalOx from *Dactilyum dendroides* by monitoring the oxygen uptake at air saturation and reported a K_S of 175 mM and a K_{O2} of 3000 μM, the last value reported as uncertain because full saturation of the enzyme could not be achieved under the experimental conditions. Moreover, the values are derived based on the ordered bi bi mechanism, an assumption that later was refuted [36,37]. A more accurate measurement of K_{O2} was carried out by Humphreys and co-workers [38] by performing the reaction at 10 °C and with $K_3Fe(CN)_6$ as activator, thereby decreasing the reaction rate and the concentration of oxygen at which enzyme saturation was observed. Under these conditions, and analyzing the oxygen concentration from 12-350 μM, the K_{O2} was determined to be 440 μM, a value much lower to the one previously reported and, even, lower than the one here reported. In the case of laccase, Gigi and co-workers [39] analyzed the enzyme from *Botritys cinerea* and compared the properties of the one obtained intracellularly with the one secreted to the external cellular medium. The K_{O2} of the extracellular and intracellular enzyme were 250 and 370 μM, respectively, in the presence of air, being these values very similar to those reported in this study. In addition, they reported that the differences in the oxidation rate of numerous phenolic substrates were not very large. For mushroom tyrosinase, Muñoz-Muñoz and co-workers [40] studied the oxidation of esculetin by a chronometric method at 25ºC and air saturation. In some cases where the o-quinones generated by polyphenol oxidases are unstable, the use of a reductant such as

ascorbic acid, which instantaneously reduces to o-quinones, has been proposed to follow the enzymatic activity, because the disappearance of the ascorbic acid can be followed spectrophotometrically. The chronometric method records the absorbance due to product formation once the ascorbic acid was consumed. They analyzed several kinetic parameters at different pH values and determined the K_{O2} at pH 4.5 and 7.0 as 41±4.1 and 40±4.0 µM, respectively.

Application of the modeling and analysis of product formation time courses.

Once the kinetic modelling was performed and constant calculated, we have summarized In Figure 10A the relationship between the operational activity of each enzyme varying the concentration of the main substrate, while an example of reaction courses over time of each enzyme is shown in Figure 10B. Both simulations were performed with data of Table 5.

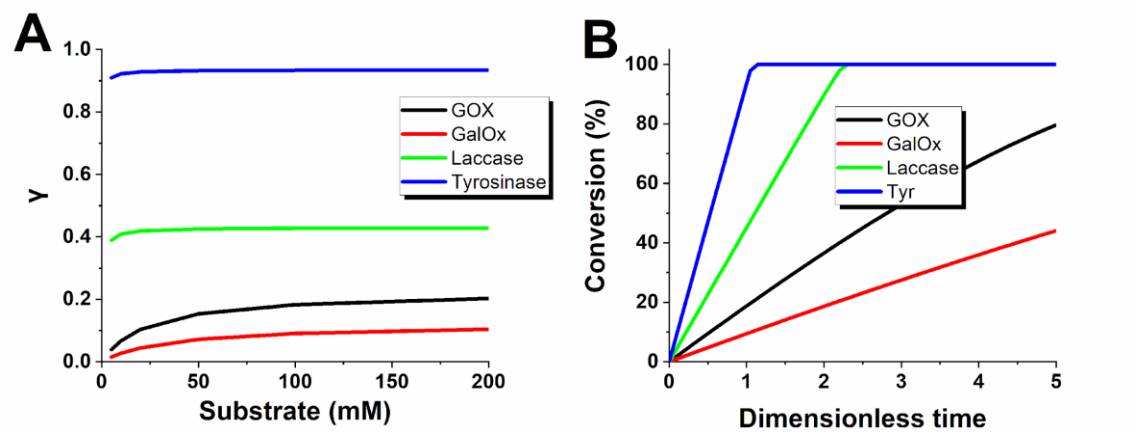

Figure 10. Analysis of operational limit and product formation time courses. Panel A: γ vs main substrate (mM). Panel B: Conversion (%) vs Dimensionless time. $[O_2]$=0.25 mM, $[S_0]$= 100 mM, $[E]$=0.1 mg/mL, Act_{max}=500 U/mg.

Figure 10A shows the maximum value of γ (Act/Act_{max}) for each enzyme, which depends on its limitation by oxygen (O_2^*), that is, at lower K_{O2}, the operational limit of the enzyme increases. On the other hand, the variation of γ with the main substrate depends on the K_S of each enzyme, so that the greater the dependence on the main substrate, that is, at higher K_S, the operational limit of the enzyme will be reached at higher concentrations. In Figure 10B it can be seen how the conversion of each enzyme varies over time and that the higher the K_{O2} and K_S constants, the slower the consumption of the substrate at the same enzyme concentration. Tyrosinase reaches the highest conversion practically in the shortest possible time since it operates almost at its maximum activity. Laccase, having a K_{O2} slightly higher than the oxygen working concentration, begins to be limited by O_2, while both GOX and GalOx are limited by both substrates, the K_S of GOX being lower than that of GalOx, and therefore, reaching higher conversions at the same time. Dimensionless time is defined in Eq 11, and it

corresponds to the ratio of operational time and characteristic reaction time, this latter is given by the time where full conversion was achieved if the reaction proceeds at maximum velocity (zero reaction order).

$$Dimensionless\ time = time \cdot \frac{V_{max}}{S_0} \qquad \textbf{Eq 11}$$

To validate the proposed kinetic model, a scaling factor of 1:100 was applied, that is, the kinetic parameters were obtained in a closed stirred vial of 5 mL, while the validation of the kinetic model was carried out at 500 mL in instrumented aerated bioreactor. In addition, this validation system is, from an industrial perspective, more suitable both from a geometric point of view (identical to tanks operated in batch in industry) and from a fluid-dynamic point of view. Oxidation of glucose by glucose oxidase was implemented in a stirred tank reactor of 500 mL of volume with continuous supply of air. First, surface aeration by using vials of 50 mL of volume and 5 mL of liquid in an end-over-end rotator was applied as preliminary assessment. Amount of enzyme was adjusted to ensure full air saturation by surface aeration. Preliminary tests are shown in Figure 11A. As next step, reactions in an instrumented stirred-tank reactor were performed. Air saturation was adjusted and controlled to two levels: 50% and 25%. Figure 11B shows the results. As can be seen in Figure 11, a very good prediction is achieved by the kinetic model to the experimental data, even varying the amount of enzyme in each experiment, thus validating the parameters of the kinetic model previously obtained.

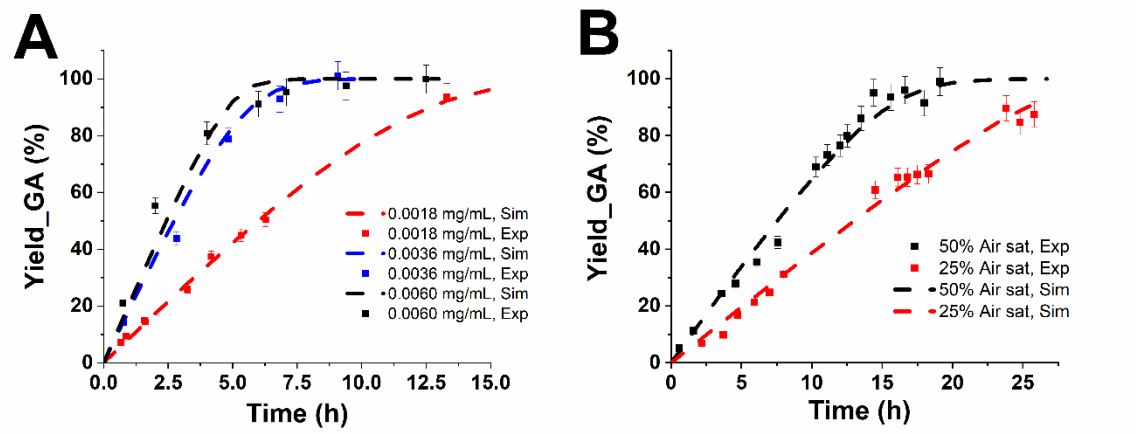

Figure 11. Selectivity towards gluconic acid vs time experiments for GOX. Panel A: with surface aeration varying the enzyme concentration $[Glucose]_0$= 100 mM, [Catalase]=0.10 mg/mL, Panel B: varying the air saturation, $[Glucose]_0$= 100 mM, [GOX]= 0.0015 mg/mL, [Catalase]=0.15 mg/mL. Simulated (dashed lines) vs experimental data (points). Yield of gluconic acid conversion (Yield_GA) is defined as the concentration of GA formed divided by $[Glucose]_0$.

To go further in the validation analysis, the same procedure was carried out for the galactose oxidase. First, oxidation of galactose by galactose oxidase by surface aeration using vials of 50 mL of volume in an end-over-end rotator was applied to choose the proper amounts of catalase and activator. Amount of enzyme was adjusted to ensure full air saturation. Then, the oxidation was implemented in a stirred tank reactor of 500 mL of volume with continuous supply of oxygen with $K_3Fe(CN)_6$ as activator for the application and validation of the kinetic modeling. Preliminary tests are shown in Figure S21. Figure 12 shows experimental and simulated time courses for that configuration. Figure 12 shows a good prediction of the kinetic model to the experimental data, thus validating the previously obtained kinetic parameters for GalOx.

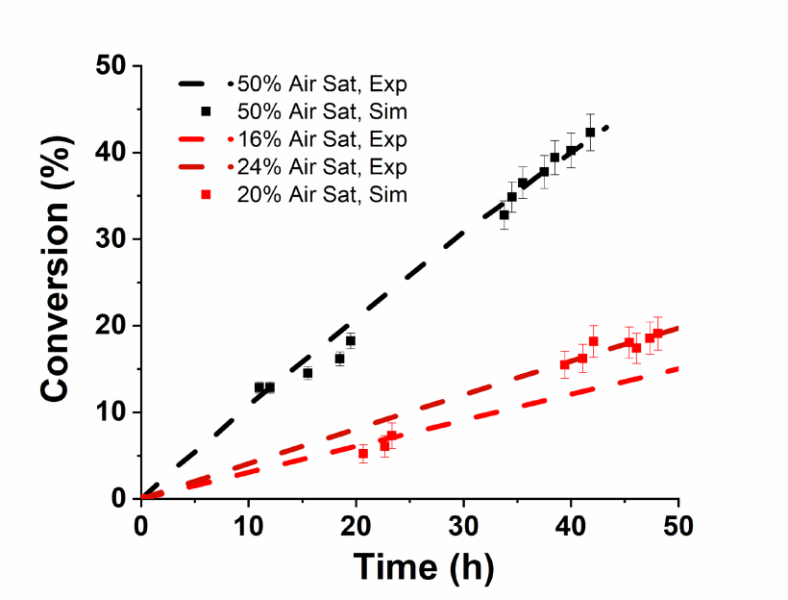

Figure 12. Conversion of galactose vs time experiments for GalOx varying the air saturation. $[Galactose]_0$= 20 mM, [GalOx]= 0.05 mg/mL, $[K_3Fe(CN)_6]$=0.05 mg/mL, [Catalase]=0.2 mg/mL. Simulated (dashed lines) vs experimental data (points).

Conclusions

A methodology has been developed and validated to quantify the kinetic parameters of bi-substrate oxygen-dependent enzyme catalysis. These kinetic parameters are interesting to identify enzyme operation opportunities and reactor intensification bottlenecks. Specifically, the parameters of the Ping-Pong bi-substrate kinetic model, K_S and K_{O2}, have been obtained for the four enzymes of interest, glucose oxidase, galactose oxidase, laccase and tyrosinase, which, in addition to their biotechnological interest, represent paradigmatic cases of study. The estimation methodology applied is based on the combination of differential methods with activity vs substrate concentration data and integral methods

with oxygen concentration vs time data. It has been studied how these kinetic parameters influence the operational limits of enzymes, being very useful when designing an industrial process to know the regions of intensification of the reaction. On the other hand, it has been shown that complex experimental facilities are not necessary when calculating the kinetic parameters of oxygen-dependent enzymes, although it is necessary to carry out numerous experiments under different conditions and a careful work of data processing. To validate the kinetic parameters, small and medium-scale experiments have been performed to predict the reaction courses of glucose and galactose oxidase. These reaction courses have been satisfactorily predicted, so the kinetic model obtained is considered validated for these enzymes and, by extension, also for laccase and tyrosinase, for having applied the same calculation procedure.

When performing the analysis of the operating windows, the enzymes with the most opportunities for intensification are those with the greatest dependence on oxygen, but they are also those with a lower operational limit (*Act/Actmax*) at saturated air conditions. It also discusses the importance of understanding the implications of reaction intensification in advanced reactor configurations [22,30,41–43] and of careful catalyst design [44–46]. Interplayed with the oxygen dependency, sufficient main substrate supply is critical for the achievement of reaction intensification and suitable production metrics (product concentration and space-time yield) [47], the achievement of enough substrate concentration is eventually limited by the solubility for which reaction engineering is integrated with kinetic modeling. Overall, the analysis framework described is also interesting because it is not only applicable to oxygen-dependent enzymes, but it can be applied to any bi-substrate enzyme system if differential and/or integral data are acquired and thanks to its easy and simple implementation it makes it even more attractive. We find it especially useful for red-ox enzymes where cofactor or redox partner (stoichiometrically consumed) must be supplied/regenerated and its concentration usually limiting.

Nomenclature

Symbols

R: Enzymatic reaction rate, mM/min

[S]: Main substrate concentration, mM

$[O_2]$: Oxygen concentration, mM

[E]: Enzyme concentration, mg/mL

Act_{max}: Maximum activity of the enzyme at saturating concentrations of both substrates, μmol/(min·mg)

Act: Enzyme activity, μmol/(min·mg)

K_S: Michaelis-Menten constant for the main substrate, mM

K_{O2}: Michaelis-Menten constant for the oxygen, mM

γ: Ratio between the enzyme activity and the maximum enzyme activity, Act/Act_{max}, -

K_{Sapp}: Michaelis-Menten apparent or observable constant for the main substrate, mM

S': Normalized concentration of substrate, S/K_S, -

O_2*: Oxygen limitation parameter, $O_2/(O_2+K_{O2})$, -

Vmax: Maximum reaction rate at saturating concentrations of both substrates, mM/min

Abbreviations

CRE: Chemical reaction engineering

GOX: Glucose oxidase

GalOx: Galactose oxidase

HRP: Horseradish peroxidase

NaPi: Sodium phosphate buffer

ABTS: 2,2'-azino-bis(3-ethylbenzothiazoline-6-sulfonic acid)

HPLC: High-performance liquid chromatography

MM: Michaelis-Menten

SQR: Sum of squared residues

RMSE: Root of mean squared errors

F: F Fisher parameter

AIC: Akaike criterion

$K_3Fe(CN)_6$: Potassium ferricyanide

GA: Gluconic acid

Acknowledgements

ALA and JMB acknowledge funding from the Government of Community of Madrid (2018-T1/BIO-10200). JMB acknowledges funding from UCM-Santander (PR108/20)

References

1. Sheldon RA: **Catalytic Oxidations in a Bio-Based Economy**. *Front Chem* 2020, **8**:132.

2. Sheldon RA, Brady D, Bode ML: **The Hitchhiker's guide to biocatalysis: recent advances in the use of enzymes in organic synthesis**. *Chem Sci* 2020, **11**:2587–2605.

3. Winkler CK, Schrittwieser JH, Kroutil W: **Power of Biocatalysis for Organic Synthesis**. *ACS Cent Sci* 2021, **7**:55–71.

4. Dong J, Fernández-Fueyo E, Hollmann F, Paul CE, Pesic M, Schmidt S, Wang Y, Younes S, Zhang W: **Biocatalytic Oxidation Reactions: A Chemist's Perspective**. *Angew Chem Int Ed* 2018, **57**:9238–9261.

5. Wu S, Snajdrova R, Moore JC, Baldenius K, Bornscheuer UT: **Biocatalysis: Enzymatic Synthesis for Industrial Applications**. *Angew Chem Int Ed* 2021, **60**:88–119.

6. Puetz H, Puchľová E, Vranková K, Hollmann F: **Biocatalytic Oxidation of Alcohols**. *Catalysts* 2020, **10**:952.

7. Bassanini I, Ferrandi EE, Riva S, Monti D: **Biocatalysis with Laccases: An Updated Overview**. *Catalysts* 2020, **11**:26.

8. Romero E, Gómez Castellanos JR, Gadda G, Fraaije MW, Mattevi A: **Same Substrate, Many Reactions: Oxygen Activation in Flavoenzymes**. *Chem Rev* 2018, **118**:1742–1769.

9. Savino S, Fraaije MW: **The vast repertoire of carbohydrate oxidases: An overview**. *Biotechnology Advances* 2020, doi:10.1016/j.biotechadv.2020.107634.

10. Woodley JM: **Reaction Engineering for the Industrial Implementation of Biocatalysis**. *Top Catal* 2019, **62**:1202–1207.

11. Doran PM: **Homogeneous Reactions**. In *Bioprocess Engineering Principles*. . Elsevier; 2013:599–703.

12. Levenspiel O: *Chemical reaction engineering*. Wiley; 1999.

13. Lindeque RM, Woodley JM: **The Effect of Dissolved Oxygen on Kinetics during Continuous Biocatalytic Oxidations**. *Org Process Res Dev* 2020, **24**:2055–2063.

14. Toftgaard Pedersen A, Birmingham WR, Rehn G, Charnock SJ, Turner NJ, Woodley JM: **Process Requirements of Galactose Oxidase Catalyzed Oxidation of Alcohols**. *Org Process Res Dev* 2015, **19**:1580–1589.

15. Meissner MP, Nordblad M, Woodley JM: **Online Measurement of Oxygen-Dependent Enzyme Reaction Kinetics**. *ChemBioChem* 2018, **19**:106–113.

16. Ringborg RH, Toftgaard Pedersen A, Woodley JM: **Automated Determination of Oxygen-Dependent Enzyme Kinetics in a Tube-in-Tube Flow Reactor**. *ChemCatChem* 2017, **9**:3285–3288.

17. Toftgaard Pedersen A, de Carvalho TM, Sutherland E, Rehn G, Ashe R, Woodley JM: **Characterization of a continuous agitated cell reactor for oxygen dependent biocatalysis:**

Biocatalytic Oxidation in a Continuous Agitated Cell Reactor. *Biotechnol Bioeng* 2017, **114**:1222–1230.

18. Nordblad M, Gomes MD, Meissner MP, Ramesh H, Woodley JM: **Scoping Biocatalyst Performance Using Reaction Trajectory Analysis**. *Org Process Res Dev* 2018, **22**:1101–1114.

19. Utikar RP, Ranade VV: **Intensifying Multiphase Reactions and Reactors: Strategies and Examples**. *ACS Sustainable Chem Eng* 2017, **5**:3607–3622.

20. Karande R, Schmid A, Buehler K: **Applications of Multiphasic Microreactors for Biocatalytic Reactions**. *Org Process Res Dev* 2016, **20**:361–370.

21. Jones E, McClean K, Housden S, Gasparini G, Archer I: **Biocatalytic oxidase: Batch to continuous**. *Chemical Engineering Research and Design* 2012, **90**:726–731.

22. Bolivar JM, Mannsberger A, Thomsen MS, Tekautz G, Nidetzky B: **Process intensification for O_2 -dependent enzymatic transformations in continuous single-phase pressurized flow**. *Biotechnology and Bioengineering* 2019, **116**:503–514.

23. Al-Haque N, Santacoloma PA, Neto W, Tufvesson P, Gani R, Woodley JM: **A robust methodology for kinetic model parameter estimation for biocatalytic reactions**. *Biotechnol Prog* 2012, **00**:11.

24. Kornecki JF, Carballares D, Tardioli PW, Rodrigues RC, Berenguer-Murcia Á, Alcántara AR, Fernandez-Lafuente R: **Enzyme production of D -gluconic acid and glucose oxidase: successful tales of cascade reactions**. *Catal Sci Technol* 2020, **10**:5740–5771.

25. Herter S, McKenna SM, Frazer AR, Leimkühler S, Carnell AJ, Turner NJ: **Galactose Oxidase Variants for the Oxidation of Amino Alcohols in Enzyme Cascade Synthesis**. *ChemCatChem* 2015, **7**:2313–2317.

26. Benítez-Mateos AI, Contente ML, Roura Padrosa D, Paradisi F: **Flow biocatalysis 101: design, development and applications**. *React Chem Eng* 2021, **6**:599–611.

27. Garcia-Ochoa F, Gomez E: **Bioreactor scale-up and oxygen transfer rate in microbial processes: An overview**. *Biotechnology Advances* 2009, **27**:153–176.

28. Pedersen AT, Rehn G, Woodley JM: **Oxygen transfer rates and requirements in oxidative biocatalysis**. In *Computer Aided Chemical Engineering*. . Elsevier; 2015:2111–2116.

29. Han S, Kashfipour MA, Ramezani M, Abolhasani M: **Accelerating gas–liquid chemical reactions in flow**. *Chem Commun* 2020, **56**:10593–10606.

30. Chapman MR, Cosgrove SC, Turner NJ, Kapur N, Blacker AJ: **Highly Productive Oxidative Biocatalysis in Continuous Flow by Enhancing the Aqueous Equilibrium Solubility of Oxygen**. *Angew Chem Int Ed* 2018, **57**:10535–10539.

31. Dias Gomes M, Woodley JM: **Considerations when Measuring Biocatalyst Performance**. *Molecules* 2019, **24**:3573.

32. Rehn G, Pedersen AT, Woodley JM: **Application of NAD(P)H oxidase for cofactor regeneration in dehydrogenase catalyzed oxidations**. *Journal of Molecular Catalysis B: Enzymatic* 2016, **134**:331–339.

33. Illanes A, Altamirano C, Wilson L: **Homogeneous Enzyme Kinetics**. In *Enzyme Biocatalysis-Principles and Applications*. . Springer; 2008:107–153.

34. **Comparison of different approaches and computer programs for progress curve analysis of enzyme kinetics**. *Eng Life Sci* 2010,

35. Kwiatkowski LD, Adelman M, Pennelly R, Kosman DJ: **Kinetic mechanism of the Cu(II) enzyme galactose oxidase**. *Journal of Inorganic Biochemistry* 1981, **14**:209–222.

36. Whittaker JW: **The radical chemistry of galactose oxidase**. *Archives of Biochemistry and Biophysics* 2005, **433**:227–239.

37. Whittaker JW: **Free Radical Catalysis by Galactose Oxidase**. *Chem Rev* 2003, **103**:2347–2364.

38. Humphreys KJ, Mirica LM, Wang Y, Klinman JP: **Galactose Oxidase as a Model for Reactivity at a Copper Superoxide Center**. *J Am Chem Soc* 2009, **131**:4657–4663.

39. Gigi O, Marbach I, Mayer AM: **Properties of gallic acid-induced extracellular laccase of Botrytis cinerea**. *Phytochemistry* 1981, **20**:1211–1213.

40. Munoz-Munoz JL, Garcia-Molina F, Varon R, Rodriguez-Lopez JN, Garcia-Canovas F, Tudela J: **Kinetic Characterization of the Oxidation of Esculetin by Polyphenol Oxidase and Peroxidase**. *Bioscience, Biotechnology, and Biochemistry* 2007, **71**:390–396.

41. Bolivar JM, Schelch S, Pfeiffer M, Nidetzky B: **Intensifying the O2-dependent heterogeneous biocatalysis: Superoxygenation of solid support from H2O2 by a catalase tailor-made for effective immobilization**. *Journal of Molecular Catalysis B: Enzymatic* 2016, **134**:302–309.

42. Illner S, Hofmann C, Löb P, Kragl U: **A Falling-Film Microreactor for Enzymatic Oxidation of Glucose**. *ChemCatChem* 2014, **6**:1748–1754.

43. Cosgrove SC, Mattey AP, Riese M, Chapman MR, Birmingham WR, Blacker AJ, Kapur N, Turner NJ, Flitsch SL: **Biocatalytic Oxidation in Continuous Flow for the Generation of Carbohydrate Dialdehydes**. *ACS Catal* 2019, **9**:11658–11662.

44. Bolivar JM, Consolati T, Mayr T, Nidetzky B: **Quantitating intraparticle O $_2$ gradients in solid supported enzyme immobilizates: Experimental determination of their role in limiting the catalytic effectiveness of immobilized glucose oxidase**. *Biotechnol Bioeng* 2013, **110**:2086–2095.

45. Bolivar JM, Nidetzky B: **The Microenvironment in Immobilized Enzymes: Methods of Characterization and Its Role in Determining Enzyme Performance**. *Molecules* 2019, **24**:3460.

46. Bolivar JM, Schelch S, Mayr T, Nidetzky B: **Dissecting Physical and Biochemical Factors of Catalytic Effectiveness in Immobilized D -Amino Acid Oxidase by Real-Time Sensing of O $_2$ Availability Inside Porous Carriers**. *ChemCatChem* 2014, **6**:981–986.

47. Domínguez de María P: **Biocatalysis, sustainability, and industrial applications: Show me the metrics**. *Current Opinion in Green and Sustainable Chemistry* 2021, **31**:100514.